

## Chapter 12

# Analytic approach for dissipative semiclassical Rabi model under parametric modulation

A. Marinho<sup>1,2,a</sup> and A. Dodonov<sup>2,3,b</sup>

<sup>1</sup> Universidade Federal Rural da Amazônia, Campus de Parauapebas, Parauapebas, PA, Brazil

<sup>2</sup> International Center of Physics, University of Brasilia, Brasilia, DF, Brazil

<sup>3</sup> Institute of Physics, University of Brasilia, Brasilia, DF, Brazil

E-mail: (a) adnei@ufra.edu.br; (b) adodonov@unb.br

### 12.1 Introduction

The paradigmatic case of a two-level fermionic system interacting with a single bosonic mode, such as the dipole interaction between a two-level atom (qubit) and the Electromagnetic (EM) field confined in a single-mode cavity, is described by the celebrated Quantum Rabi Model [1–3] (we set  $\hbar = 1$ )

$$\hat{H}_R(t) = \omega \hat{a}^\dagger \hat{a} + \frac{\Omega}{2} \hat{\sigma}_z + g_1 (\hat{a} + \hat{a}^\dagger) (\hat{\sigma}_+ + \hat{\sigma}_-), \quad (12.1)$$

where  $\hat{a}$  and  $\hat{a}^\dagger$  are the cavity annihilation and creation operators and  $\hat{\sigma}_+ = |e\rangle\langle g|$ ,  $\hat{\sigma}_- = |g\rangle\langle e|$ ,  $\hat{\sigma}_z = |e\rangle\langle e| - |g\rangle\langle g|$  are the atomic Pauli operators.  $|g\rangle$  ( $|e\rangle$ ) denotes the atomic ground (excited) state,  $\omega$  is the cavity frequency,  $\Omega$  is the atomic transition frequency and  $g_1$  is the atom–field coupling strength. When one or several system parameters are modulated externally as  $X = X_0 + \varepsilon_X \sin(\eta t + \phi_X)$  (where  $X_0$  is the bare value of  $X$ )

in the absence of modulation,  $\varepsilon_X \ll X_0$  is the modulation amplitude,  $\eta$  is the frequency of perturbation and  $\phi_X$  is the phase), for certain values of  $\eta$  the system can undergo coherent transitions between the dressed-states (eigenstates of  $\hat{H}_R$  when  $\varepsilon_X = 0$ ) [4–7]. In particular, in the dispersive regime (when  $|\omega - \Omega| \gg g_1 \sqrt{n}$  for all the populated cavity Fock states  $|n\rangle$ ) the system can exhibit the following behaviors:

- *Odd-photon exchange transition*  $|g, n\rangle \leftrightarrow |e, n - k\rangle$  ( $k = 1, 3, \dots$ ) within the reduced subspace  $\{|g, n\rangle, |e, n\rangle\}$ ,  $n \in [n_{\min}, n_{\max}]$ , described by the effective Jaynes-Cummings Hamiltonian with the additional ac Stark shift [6, 9–12]

$$\hat{H}_{k,e} \propto \hat{a}^k \hat{\sigma}_+ + \hat{a}^{\dagger k} \hat{\sigma}_- + \delta_{\text{ac}} \hat{a}^\dagger \hat{a} \hat{\sigma}_z. \quad (12.2)$$

- *Odd-photon creation transition*  $|g, n\rangle \leftrightarrow |e, n + k\rangle$  ( $k = 1, 3, \dots$ ) within the reduced subspace  $\{|g, n\rangle, |e, n\rangle\}$ ,  $n \in [n_{\min}, n_{\max}]$ , described by the effective anti-Jaynes-Cummings Hamiltonian with ac Stark shift [6, 9–12]

$$\hat{H}_{k,c} \propto \hat{a}^k \hat{\sigma}_- + \hat{a}^{\dagger k} \hat{\sigma}_+ + \delta_{\text{ac}} \hat{a}^\dagger \hat{a} \hat{\sigma}_z. \quad (12.3)$$

- *Even-photon creation transition*  $|g, n\rangle \leftrightarrow |g, n \pm k\rangle$  and/or  $|e, n\rangle \leftrightarrow |e, n \pm k\rangle$  ( $k = 2, 4, \dots$ ) within some reduced subspace  $\{|g, n\rangle, |e, n\rangle\}$ ,  $n \in [n_{\min}, n_{\max}]$ , described by the effective  $k$ -photon parametric amplification Hamiltonian with the additional Kerr shift [5, 13, 14]

$$\hat{H}_{k,pa} \propto \hat{a}^k + \hat{a}^{\dagger k} + \delta_{\text{Kerr}} (\hat{a}^\dagger \hat{a})^2. \quad (12.4)$$

More complex phenomena can be induced by employing multi-level atoms instead of qubits and/or multi-mode cavities instead of single-mode ones, for example: even-photon exchange and creation transitions, odd-photon effective parametric amplification, excitation of the atom without changing the photon number, generation of multipartite entangled states, extraction of work from a thermal reservoir, multi-squeezed state generation, multiphoton bundle emission, etc [6–8, 13, 15–22].

Since the odd-photon exchange and creation transitions (12.2) and (12.3) cause excitation and deexcitation of the qubit for an arbitrary number of photons, the phenomenon should persist for arbitrary large values of  $n$ . In particular, it must hold for the cavity field in the large-amplitude coherent state  $|\alpha\rangle$  with  $\alpha \gg 1$  (without loss of generality we assume that  $\alpha$  is real). In this case, the depletion of the intensity of the cavity field is negligible and one can treat it as classical. To obtain the semiclassical Hamiltonian we can first go to the interaction picture with respect to the cavity field, so the interaction-picture Hamiltonian (12.1) reads

$$\hat{H}_I(t) = \frac{\Omega}{2} \hat{\sigma}_z + g_1 (\hat{a} e^{-it\omega} + \hat{a}^\dagger e^{it\omega}) (\hat{\sigma}_+ + \hat{\sigma}_-). \quad (12.5)$$

Now, assuming that changes in the cavity field state are negligible (i. e., for  $\alpha \gg 1$ ), one can approximate the dynamics by imposing that the EM field remains in the same state  $|\alpha\rangle$  throughout the evolution. Evaluating the partial trace over the cavity field, one gets the atomic Hamiltonian [23, 24]

$$\begin{aligned} \hat{H}(t) &= \text{Tr}_f \left[ |\alpha\rangle \langle \alpha| \hat{H}_I(t) \right] = \frac{\Omega}{2} \hat{\sigma}_z + g_1 \alpha (e^{-it\omega} + e^{it\omega}) (\hat{\sigma}_+ + \hat{\sigma}_-) \\ &= \frac{\Omega}{2} \hat{\sigma}_z + 2g \cos \omega t (\hat{\sigma}_+ + \hat{\sigma}_-), \end{aligned} \quad (12.6)$$

where we defined the semiclassical coupling constant  $g = g_1\alpha$ . A more rigorous description of how the semiclassical Rabi model emerges from the quantum one can be found in [25].

Eq. (12.6) is precisely the Hamiltonian used originally by Rabi and later by Bloch and others to describe the matter interaction with classical EM fields [26–28]. Thus, the excitation of the two-level system by a far detuned laser field of frequency  $\omega$  (i. e., for  $|\omega - \Omega| \gg g$ ) due to resonant modulation of  $\Omega$  or/and  $g$  must be hidden in this simple, almost ninety years old Hamiltonian [2]. In this chapter we confirm this hint and present a detailed step by step derivation of the system dynamics in the presence of Markovian dissipation and harmonic modulation of the atomic transition frequency  $\Omega$ . In particular, we calculate the resonant frequencies and the associated transition rates for the 1-, 3- and 5-photon transitions.

## 12.2 Dressed-states expansion

We consider the dissipative two-level system (qubit) interacting with a classical EM field via the dipole interaction [23–25, 29]. Assuming the standard Markovian damping and dephasing of the qubit due to thermal reservoirs, the system dynamics is governed by the “standard” master equation [35, 36] (recalling that  $\hbar = 1$ )

$$\begin{aligned} \frac{\partial \hat{\rho}}{\partial t} = & -i \left[ \hat{H}(t), \hat{\rho} \right] + \gamma_\phi (\hat{\sigma}_z \hat{\rho} \hat{\sigma}_z - \hat{\rho}) \\ & + \frac{\gamma}{2} (n_t + 1) (2\hat{\sigma}_- \hat{\rho} \hat{\sigma}_+ - \hat{\sigma}_+ \hat{\sigma}_- \hat{\rho} - \hat{\rho} \hat{\sigma}_+ \hat{\sigma}_-) + \frac{\gamma}{2} n_t (2\hat{\sigma}_+ \hat{\rho} \hat{\sigma}_- - \hat{\sigma}_- \hat{\sigma}_+ \hat{\rho} - \hat{\rho} \hat{\sigma}_- \hat{\sigma}_+) , \end{aligned} \quad (12.7)$$

where  $\hat{\rho}$  is the density operator and the time-dependent Hamiltonian is

$$\hat{H}(t) = \frac{\Omega_0 + \varepsilon f(t)}{2} \hat{\sigma}_z + 2g \cos \omega t (\hat{\sigma}_+ + \hat{\sigma}_-) . \quad (12.8)$$

In Eq. (12.7)  $\Omega_0$  is the bare atomic frequency,  $\varepsilon \ll \Omega_0$  is the modulation depth,  $f(t) = \sin \eta t$  is the externally prescribed modulation with the modulation frequency  $\eta > 0$ ,  $g > 0$  is the semiclassical light-matter coupling constant,  $\omega$  is the laser frequency,  $\gamma$  is the damping rate,  $\gamma_\phi$  is the pure dephasing rate and  $n_t = [e^{\hbar\Omega_0/k_B T} - 1]^{-1}$  is the average thermal photon number for the reservoir’s temperature  $T$ . Our goal is to present a simple analytic method for obtaining closed approximate expressions for the density matrix  $\hat{\rho}$  in the *dispersive regime* ( $|\omega - \Omega_0| \gg g$ ) when the modulation frequency  $\eta$  matches the resonance conditions. Analytic approaches for the semiclassical Rabi model in other scenarios can be found in [29–34] and references therein.

First we perform the unitary transformation

$$\hat{\rho} = \hat{U}_t \hat{\rho}_1 U_t^\dagger , \quad \hat{U}_t = \exp \left( -\frac{i\omega t}{2} \hat{\sigma}_z \right) \quad (12.9)$$

to obtain the master equation for  $\hat{\rho}_1$

$$\begin{aligned} \frac{\partial \hat{\rho}_1}{\partial t} = & -i \left( \hat{H}_{ef} \hat{\rho}_1 - \hat{\rho}_1 \hat{H}_{ef}^\dagger \right) - i \left[ \frac{\varepsilon f}{2} \hat{\sigma}_z + g (\hat{\sigma}_+ e^{i2\omega t} + \hat{\sigma}_- e^{-i2\omega t}) , \hat{\rho}_1 \right] + \gamma_\phi \hat{\sigma}_z \hat{\rho}_1 \hat{\sigma}_z \\ & + \frac{\gamma}{2} (n_t + 1) (2\hat{\sigma}_- \hat{\rho}_1 \hat{\sigma}_+ - \hat{\sigma}_+ \hat{\sigma}_- \hat{\rho}_1 - \hat{\rho}_1 \hat{\sigma}_+ \hat{\sigma}_-) \\ & + \frac{\gamma}{2} n_t (2\hat{\sigma}_+ \hat{\rho}_1 \hat{\sigma}_- - \hat{\sigma}_- \hat{\sigma}_+ \hat{\rho}_1 - \hat{\rho}_1 \hat{\sigma}_- \hat{\sigma}_+) , \end{aligned} \quad (12.10)$$

where we defined the effective Hamiltonian

$$\hat{H}_{ef} = -\frac{\Delta_-}{2}\hat{\sigma}_z + g(\hat{\sigma}_+ + \hat{\sigma}_-) - i\gamma_\phi/2 \quad (12.11)$$

and the laser-qubit detuning

$$\Delta_- \equiv \omega - \Omega_0. \quad (12.12)$$

Our method is based on the expansion of the density matrix in terms of the orthonormal eigenstates (*dressed-states*) of  $\hat{H}_{ef}$ , which read

$$|\phi_+\rangle = \frac{R_+|g\rangle + g|e\rangle}{\sqrt{RR_+}}, \quad |\phi_-\rangle = \frac{R_-|g\rangle - g|e\rangle}{\sqrt{RR_-}}, \quad (12.13)$$

where

$$R \equiv \sqrt{\Delta_-^2 + 4g^2}, \quad R_\pm \equiv \frac{R \pm \Delta_-}{2}. \quad (12.14)$$

The corresponding eigenvalues of  $\hat{H}_{ef}$  are

$$E_\pm = \pm \frac{R}{2} - i\frac{\gamma_\phi}{2}.$$

The next step is to expand the density operator as

$$\begin{aligned} \hat{\rho}_1 = & e^{-t\gamma_\phi} [A(t)|\phi_+\rangle\langle\phi_+| + (e^{t\gamma_\phi} - A(t))|\phi_-\rangle\langle\phi_-| \\ & + e^{-itR}C(t)|\phi_+\rangle\langle\phi_-| + e^{itR}C^*(t)|\phi_-\rangle\langle\phi_+|], \end{aligned} \quad (12.15)$$

where  $A$  and  $C$  are time-dependent coefficients whose analytic expressions are the main goal of this work. Once they are found, the atomic excitation probability and the average value of  $\hat{\sigma}_-$ , which also fully characterize the system dynamics, are determined from

$$P_e = \text{Tr}[\hat{\rho}|e\rangle\langle e|] = \frac{g^2}{RR_-} - \frac{e^{-t\gamma_\phi}}{R} [\Delta_-A + 2g\text{Re}(e^{-itR}C)]. \quad (12.16)$$

$$\langle\sigma_-\rangle = \text{Tr}[\hat{\rho}\hat{\sigma}_-] = \frac{e^{-i\omega t}e^{-t\gamma_\phi}}{R} [g(2A - e^{t\gamma_\phi}) + R_-e^{-itR}C - R_+e^{itR}C^*]. \quad (12.17)$$

For future use, we also write down the relation among  $A$  and  $C$  implied by the condition  $\text{Tr}[\hat{\rho}^2] \leq 1$ :

$$|C(t)|^2 \leq A(t)(e^{t\gamma_\phi} - A(t)). \quad (12.18)$$

So far all the equations were exact. But from now on we assume the realistic case of *weak dissipation and large detuning*

$$\diamond \text{ Approximation 1: } \quad g \ll |\Delta_-|, \omega \quad ; \quad \gamma_\phi, \gamma(n_t + 1) \ll \frac{\Delta_-^2}{g}, \omega. \quad (12.19)$$

From (12.10) we obtain the approximate equations governing the evolution of  $A$  and  $C$

$$\dot{A} \approx i\frac{g}{R} [M_\varepsilon e^{-itR}C - c.c.] + \Gamma_1 A + L e^{t\gamma_\phi} \quad (12.20)$$

$$\dot{C} \approx -\Gamma_2 C + \frac{i}{R} [(\varepsilon f \Delta_- - 4g^2 \cos 2\omega t) C + g M_\varepsilon^* e^{itR} (2A - e^{t\gamma_\phi})], \quad (12.21)$$

where *c.c.* denotes the complex conjugate and we defined

$$M_\varepsilon \equiv R_- e^{-it2\omega} - \varepsilon f - R_+ e^{it2\omega}, \quad M_0 \equiv M_{\varepsilon=0} \quad (12.22)$$

$$\Gamma_1 \equiv \gamma_\phi (1 - 8\zeta^2) - 2\gamma \left( n_t + \frac{1}{2} \right) (1 - 2\zeta^2) \quad (12.23)$$

$$\Gamma_2 \equiv \gamma_\phi (1 - 4\zeta^2) + \gamma \left( n_t + \frac{1}{2} \right) (1 + 2\zeta^2) \quad (12.24)$$

$$\Gamma_3 \equiv \Gamma_1 + \Gamma_2 = \left[ 2\gamma_\phi - \gamma \left( n_t + \frac{1}{2} \right) \right] (1 - 6\zeta^2) \quad (12.25)$$

$$\Gamma_4 = \Gamma_1 - \gamma_\phi, \quad \Gamma_5 = \Gamma_2 + \gamma_\phi \quad (12.26)$$

$$L \equiv 4\zeta^2 \gamma_\phi + \gamma \left( n_t + \frac{1 + \mathcal{D}}{2} \right) (1 - 2\zeta^2) \quad (12.27)$$

$$\zeta \equiv \frac{g}{\Delta_-}, \quad \mathcal{D} \equiv \text{sign}(\Delta_-) = \pm 1. \quad (12.28)$$

## 12.3 First transformation

In our quest for a closed analytic solution, first we define

$$\star \text{ 1st Transformation: } A(t) = A_1(t) e^{t\Gamma_1}, \quad C(t) = C_1(t) e^{iq} W_1(t) W_2(t) e^{-t\Gamma_2}, \quad (12.29)$$

where  $A_1(0) = A(0)$ ,  $C_1(0) = C(0)$  and

$$W_1(t) \equiv \exp[-iq \cos \eta t] \quad (12.30)$$

$$W_2(t) \equiv \exp[-iq_2 \cos(2\omega t - \pi/2)] \quad (12.31)$$

$$q \equiv \frac{\varepsilon \Delta_-}{\eta R}, \quad q_2 \equiv \frac{2g^2}{\omega R}. \quad (12.32)$$

Now we use the Jacobi-Anger expansion

$$e^{iZ \cos \theta} = J_0(Z) + \sum_{m=1}^{\infty} i^m J_m(Z) (e^{im\theta} + e^{-im\theta}), \quad (12.33)$$

where  $J_m(Z)$  is the Bessel function of the first kind. For the additional approximation

$$\diamond \text{ Approximation 2: } \varepsilon \ll \eta \quad (12.34)$$

we obtain the equations

$$\dot{A}_1 = i e^{-t\Gamma_3} \frac{g}{R} \{[(\Pi_{00} - 2h_t) M_0 - \varepsilon f W_1 W_2] C_1 e^{iq} e^{-itR} - \text{c.c.}\} + L e^{-t\Gamma_4} \quad (12.35)$$

$$\dot{C}_1 = i \frac{g}{R} e^{-iq} e^{itR} (\Pi_{00} - 2h_t^*) M_\varepsilon^* (2A_1 e^{t\Gamma_3} - e^{t\Gamma_5}) \quad (12.36)$$

with the short-hand notations

$$\Pi_{ij} \equiv J_i(q) J_j(q_2) \quad (12.37)$$

$$h_t \equiv i\Pi_{01} \sin 2\omega t + i\Pi_{10} \cos \eta t + 2\Pi_{11} \sin 2\omega t \cos \eta t. \quad (12.38)$$

We note that in this work we do not take into account the terms proportional to  $J_m(q)$  and  $J_m(q_2)$  with  $m > 1$  in the expansion (12.33), although they can be taken into account in a straightforward (but cumbersome) manner.

## 12.4 Second auxiliary transformation

To solve (12.35) – (12.36) it is convenient to make an additional auxiliary transformation, which will be crucial for proposing the definitive ansatz in the next section. The trick is to solve the auxiliary equations

$$\dot{A}_1 = ie^{-t\Gamma_3} \frac{g\Pi_{00}}{R} [M_0 C_1 e^{iq} e^{-itR} - c.c.] \quad (12.39)$$

$$\dot{C}_1 = i \frac{g\Pi_{00}}{R} e^{-iq} e^{itR} M_0^* (2A_1 e^{t\Gamma_3} - e^{t\Gamma_5}) \quad (12.40)$$

obtained from (12.35) – (12.36) by setting formally  $f = h_t = L = 0$ . Since in the dispersive regime we have

$$R \approx \mathcal{D}(\Delta_- + 2\delta_-) , \quad (12.41)$$

where

$$\delta_- = \frac{g^2}{\Delta_-} \quad (12.42)$$

is the standard *dispersive shift*, Eqs. (12.39) - (12.40) become

$$\dot{A}_1 \approx -e^{-t\Gamma_3} [G e^{itY} C_1 + c.c.] \quad (12.43)$$

$$\dot{C}_1 \approx G^* e^{-itY} (2A_1 e^{t\Gamma_3} - e^{t\Gamma_5}) \quad (12.44)$$

with

$$G \equiv \text{Dig}\Pi_{00} e^{iq} , \quad Y \equiv \mathcal{D}(2\omega - \mathcal{D}R) . \quad (12.45)$$

Now we do the second transformation by defining

$$\star \text{ 2}^{\text{nd}} \text{ auxiliary Transformation: } A_1(t) = A_2(t) e^{-t\Gamma_3/2}, \quad C_1(t) = C_2(t) e^{t\Gamma_3/2}, \quad (12.46)$$

where  $A_2$  and  $C_2$  are time-dependent functions obeying the initial conditions  $A_2(0) = A(0)$  and  $C_2(0) = C(0)$ . After substituting (12.46) into (12.43) - (12.44) we obtain

$$\dot{A}_2 \approx - (G e^{itY} C_2 + c.c.) + \Gamma_3 A_2 / 2 \quad (12.47)$$

$$\dot{C}_2 \approx G^* e^{-itY} (2A_2 - e^{tz}) - \Gamma_3 C_2 / 2 , \quad (12.48)$$

where

$$z \equiv \Gamma_5 - \Gamma_3/2 = \gamma_\phi (1 + 2\zeta^2) + \gamma \left( n_t + \frac{1}{2} \right) \left( \frac{3}{2} - \zeta^2 \right) . \quad (12.49)$$

Deriving  $\dot{C}_2$  once more with time we get

$$\ddot{C}_2 + iY\dot{C}_2 + \left[ iY\Gamma_3/2 + 2(|G|^2 - \Gamma_3^2/8) \right] C_2 + 2G^{2*} e^{-2itY} C_2^* \approx \left( \frac{\Gamma_3}{2} - z \right) G^* e^{t(z-iY)} , \quad (12.50)$$

where

$$\left( \frac{\Gamma_3}{2} - z \right) = -\gamma_\phi 8\zeta^2 - 2\gamma \left( n_t + \frac{1}{2} \right) (1 - 2\zeta^2) . \quad (12.51)$$

Now we perform the most important physical assumption in our deduction – *the coarse-grained approximation*, which requires that the rate of change of  $C_2$  (and therefore of  $C_1$ ) is much smaller than  $\omega$ :

$$\diamond \text{ Approximation 3: } \quad \text{rate of change of } C_1 \ll \omega. \quad (12.52)$$

So instead of studying the instantaneous dynamics, we focus on the blurred (coarse-grained) evolution averaged over the time-scale  $2\pi/Y$ .

Averaging both sides of (12.50) over one characteristic period  $T_Y = 2\pi Y^{-1}$  we get

$$\begin{aligned} & \frac{1}{T_Y} \int_t^{t+T_Y} dt' \left[ \ddot{C}_2 + iY\dot{C}_2 + \left[ iY\Gamma_3/2 + 2 \left( |G|^2 - \Gamma_3^2/8 \right) \right] C_2 + 2G^{2*} e^{-2it'Y} C_2^* \right] \\ & \approx \frac{1}{T_Y} \left( \frac{\Gamma_3}{2} - z \right) \int_t^{t+T_Y} dt' G^* e^{t'(z-iY)}. \end{aligned} \quad (12.53)$$

Since  $C_2$  and its first two derivatives are assumed to remain nearly constant on the timescale  $T_Y$ , we obtain

$$\ddot{C}_2 + iY\dot{C}_2 + \left[ iY\Gamma_3/2 + 2 \left( |G|^2 - \Gamma_3^2/8 \right) \right] C_2 \approx \varkappa e^{t(z-iY)}, \quad (12.54)$$

where

$$\varkappa = G^* (\Gamma_3/2 - z) \frac{Y}{(z - iY)} \frac{e^{2\pi z/Y} - 1}{2\pi} = \mathcal{O} \left( (\Gamma_3/2 - z) z \frac{g}{\omega} \right). \quad (12.55)$$

The particular solution of (12.54) is

$$C_2^{(part)} = \frac{\varkappa}{z^2 + i(\Gamma_3/2 - z)Y + 2 \left( |G|^2 - \Gamma_3^2/8 \right)} e^{t(z-iY)}. \quad (12.56)$$

The homogeneous solution can be found trivially, so the general solution of (12.54) reads

$$C_2 = C_2^{(part)} + C_{2,+} e^{it\gamma_+} + C_{2,-} e^{it\gamma_-}, \quad (12.57)$$

where

$$\gamma_{\pm} = \frac{-Y \pm \sqrt{(Y + i\Gamma_3)^2 + 8|G|^2}}{2}. \quad (12.58)$$

Now we must choose the solution that fulfills the requirement (12.52). This implies neglecting the terms oscillating with frequencies  $\sim Y$  and keep only the slowly oscillating terms. Therefore, we obtain

$$C_2 \approx C(0) e^{it\mathcal{D}2\delta_+} e^{-t\Gamma_3/2} \quad \Rightarrow \quad C_1 = C(0) e^{it\mathcal{D}2\delta_+}, \quad (12.59)$$

where for  $|Y| \gg |G|, \Gamma_3$  we have an additional *Bloch-Siegert shift*

$$\delta_+ = \frac{|G|^2}{2\omega - \mathcal{D}R} \approx \frac{|G|^2}{\omega + \Omega_0 - \frac{2g^2}{\Delta}}. \quad (12.60)$$

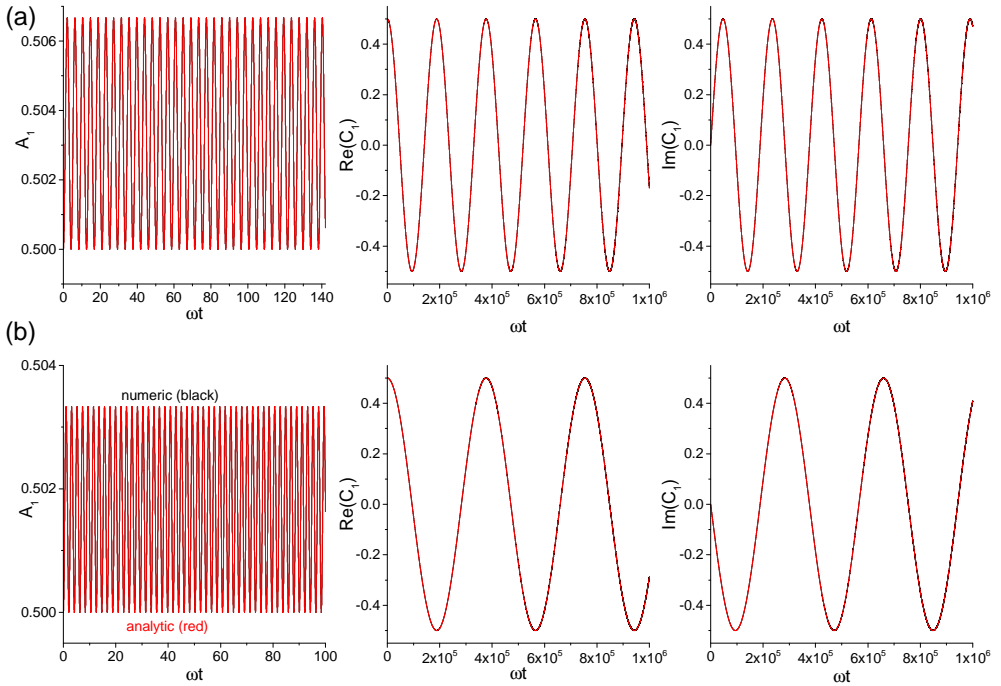


Figure 12.1: Comparison of numeric (black curves) and analytic (red curves) solutions for  $A_1$  and  $C_1$ , considering the initial conditions  $A(0) = C(0) = 1/2$  and parameters:  $g = 5 \times 10^{-3}\omega$ ,  $\gamma = 2 \times 10^{-8}\omega$ ,  $\gamma_\phi = 10^{-8}\omega$ ,  $n_t = 0.5$ ,  $\varepsilon = 10^{-2}\Omega_0$ . a) Atomic frequency  $\Omega_0 = 0.5\omega$  ( $\mathcal{D} = +1$ ). b) Atomic frequency  $\Omega_0 = 2\omega$  ( $\mathcal{D} = -1$ ). No discrepancies can be observed within the widths of the curves.

From (12.47) we find

$$\dot{A}_2 - \frac{\Gamma_3}{2}A_2 \approx - \left( C(0) G e^{it(Y + \mathcal{D}2\delta_+ + i\Gamma_3/2)} + C^*(0) G^* e^{-it(Y + \mathcal{D}2\delta_+ - i\Gamma_3/2)} \right). \quad (12.61)$$

Using the approximate solution (12.59) we find immediately

$$A_2 = \left\{ A(0) + i \left[ C(0) G \frac{e^{it(Y + \mathcal{D}2\delta_+ + i\Gamma_3)} - 1}{Y + \mathcal{D}2\delta_+ + i\Gamma_3} - C^*(0) G^* \frac{e^{-it(Y + \mathcal{D}2\delta_+ - i\Gamma_3)} - 1}{Y + \mathcal{D}2\delta_+ - i\Gamma_3} \right] \right\} e^{t\Gamma_3/2} \quad (12.62)$$

hence

$$A_1 = A(0) + 2\text{Im} \left( C(0) \frac{ig\Pi_{00}e^{iq}}{(2\omega + 2\delta_+ - \mathcal{D}R) + i\mathcal{D}\Gamma_3} \right) - 2\text{Im} \left( C(0) \frac{G}{Y + \mathcal{D}2\delta_+ + i\Gamma_3} e^{it(Y + \mathcal{D}2\delta_+)} e^{-t\Gamma_3} \right) \quad (12.63)$$

To test the validity of our approximations, in Figure 12.1 we solved numerically the complete equations (12.39) - (12.40) and compared the results to the approximate solutions (12.59) and (12.63). For the sake of illustration, we considered the initial conditions

$A(0) = C(0) = 1/2$  [satisfying the inequality (12.18)] and parameters:  $g = 5 \times 10^{-3}\omega$ ,  $\gamma = 2 \times 10^{-8}\omega$ ,  $\gamma_\phi = 10^{-8}\omega$ ,  $n_t = 0.5$ ,  $\varepsilon = 10^{-2}\Omega_0$ ,  $\Omega_0 = 0.5\omega$  (panel 12.1a,  $\mathcal{D} = +1$ ) and  $\Omega_0 = 2\omega$  (panel 12.1b,  $\mathcal{D} = -1$ ). We see an excellent agreement: the exact numerical results (black curves) are indistinguishable from the approximate analytic results (red curves) within the widths of the lines. Since the rapidly oscillating term in (12.63) is small due to the assumption (12.19), we perform an additional approximation

$$\diamond \text{ Approximation 4: } \quad \text{rate of change of } A_1 \ll \omega \quad (12.64)$$

that allows us to neglect the third term on the RHS of (12.63) by averaging  $A_1$  over the time interval  $T_Y$ ; we also neglect the second term, since it is of the order  $\sim gC(0)/\omega$ . Therefore, *under the coarse-grained approximations both for  $A_1$  and  $C_1$* , combined with the assumptions (12.19) and (12.34), the solution of equations (12.39) - (12.40) is

$$A_1(t) = A(0) \quad , \quad C_1(t) = C(0) e^{it\mathcal{D}2\delta_+} . \quad (12.65)$$

The analysis made in this section also makes clear that whenever one neglects completely the ‘‘rapidly oscillating terms’’ in equations of the type (12.39) - (12.40), setting the RHS formally to zero, one ends up missing a small frequency shift (of the order of  $\delta_+$ ) in the phase of the coefficient  $C_1$  (therefore, committing a small error in the prediction of resonant modulation frequencies) [4]. This can be seen from the solution (12.65), whose RHS is zero only if one neglects the frequency shift  $\mathcal{D}2\delta_+$ .

## 12.5 Third transformation

Now we make the third and final transformation

$$\star \text{ 3<sup>rd</sup> Transformation: } \quad A_1(t) = A_3(t) \quad , \quad C_1(t) = C_3(t) e^{iq} e^{it\mathcal{D}2\delta_+} , \quad (12.66)$$

where the unknown functions  $A_3(t)$  and  $C_3(t)$  have rates of change small compared to  $\omega$  (due to the coarse-grained approximation of the previous section), and satisfy the initial conditions  $A_3(0) = A(0)$  and  $C_3(0) = C(0) e^{-iq}$ . By substituting (12.66) into equations (12.35)–(12.36), the terms contained on the RHS of the equations (12.39) – (12.40) are automatically eliminated and one is left with the equations

$$\dot{A}_3 \approx -i \frac{g}{R} \left[ (\varepsilon f \Pi_{00} + 2M_\varepsilon h_t) e^{-it(R-2\mathcal{D}\delta_+)} C_3 - c.c. \right] e^{-it\Gamma_3} + L e^{-it\Gamma_4} \quad (12.67)$$

$$\dot{C}_3 \approx -i \frac{g}{R} (\varepsilon f \Pi_{00} + 2M_\varepsilon h_t)^* e^{it(R-2\mathcal{D}\delta_+)} \left[ 2A_3 e^{it\Gamma_3} - e^{it\Gamma_5} \right] . \quad (12.68)$$

Our method is self-consistent provided  $A_3$  and  $C_3$  vary slowly with time, which can only occur for a discrete set of *resonant modulation frequencies* for which the RHS of (12.67) - (12.68) contain slowly oscillating terms (whence all the rapidly oscillating terms can be neglected at the cost of introducing small uncertainties in the analytic prediction of the resonant frequencies).

## 12.6 1-, 3- and 5-photon resonances

By neglecting the rapidly oscillating terms, after lengthy but straightforward calculations one obtains the general equations

$$\dot{A}_3 = \chi_n \left[ e^{itS_n(\varpi_n - \eta)} C_3 + c.c. \right] e^{-t\Gamma_3} + L e^{-t\Gamma_4} \quad (12.69)$$

$$\dot{C}_3 = -\chi_n e^{-itS_n(\varpi_n - \eta)} [2A_3 e^{t\Gamma_3} - e^{t\Gamma_5}] , \quad (12.70)$$

where  $\chi_n$  (a real function) and  $\varpi_n$  are the transition rate and the resonant frequency associated with the  $n$ -th allowed transition, respectively, while  $S_n = \pm 1$  is some unimportant sign typical of each resonance. Considering only the linear terms in the modulation depth  $\varepsilon$ , the five strongest transitions are:

- *1-photon exchange transition*: quantum mechanically, this corresponds to the Jaynes-Cummings transition described by the effective interaction Hamiltonian  $\hat{a}^\dagger \hat{\sigma}_- + h.c.$

$$\begin{aligned} \chi_{1,e} &= -\frac{g\varepsilon\Pi_{00}}{2R} \\ \mathcal{S}_{1,e} &= -1 \\ \varpi_{1,e} &= R - 2\mathcal{D}\delta_+ . \end{aligned} \quad (12.71)$$

- *1-photon creation transition*: corresponds to the anti-Jaynes-Cummings transition described by the effective interaction Hamiltonian  $\hat{a}^\dagger \hat{\sigma}_+ + h.c.$

$$\begin{aligned} \chi_{1,c} &= -\frac{g}{R} \left( \mathcal{D}R_{\mathcal{D}}\Pi_{10} + \varepsilon\frac{\Pi_{01}}{2} \right) \\ \mathcal{S}_{1,c} &= \mathcal{D} \\ \varpi_{1,c} &= 2\omega + 2\delta_+ - \mathcal{D}R \approx \omega + \Omega_0 - 2(\delta_- - \delta_+) . \end{aligned} \quad (12.72)$$

- *3-photon exchange transition*: corresponds to the 3-photon Jaynes-Cummings transition described by the effective interaction Hamiltonian  $\hat{a}^{\dagger 3} \hat{\sigma}_- + h.c.$

$$\begin{aligned} \chi_{3,e} &= \frac{g}{R} \left( \mathcal{D}R_{-\mathcal{D}}\Pi_{10} - \mathcal{D}_2\varepsilon\frac{\Pi_{01}}{2} \right) \\ \mathcal{S}_{3,e} &= -\mathcal{D}_2\mathcal{D} , \quad \mathcal{D}_2 \equiv \text{sign}(2\omega - 2\delta_+ - R) \\ \varpi_{3,e} &= |2\omega - 2\delta_+ + \mathcal{D}R| \approx |3\omega - \Omega_0 + 2(\delta_- - \delta_+)| . \end{aligned} \quad (12.73)$$

This effect was also called "Anti-dynamical Casimir effect" in [5], since it can lead to coherent annihilation of excitations from the initial thermal state of the cavity field [11, 17, 18, 21, 22, 37].

- *3-photon creation transition*: corresponds to the 3-photon anti-Jaynes-Cummings transition described by the effective interaction Hamiltonian  $\hat{a}^{\dagger 3} \hat{\sigma}_+ + h.c.$

$$\begin{aligned} \chi_{3,c} &= \frac{gR_{\mathcal{D}}\Pi_{11}}{R} + (\text{corr.}) \\ \mathcal{S}_{3,c} &= \mathcal{D} \\ \varpi_{3,c} &= 4\omega + 2\delta_+ - \mathcal{D}R \approx 3\omega + \Omega_0 - 2(\delta_- - \delta_+) , \end{aligned} \quad (12.74)$$

where (corr.) denote additional terms proportional to the Bessel functions  $J_2(q)$  and  $J_2(q_2)$ .

- *5-photon exchange transition*: corresponds to the 5-photon Jaynes-Cummings transition described by the effective interaction Hamiltonian  $\hat{a}^{\dagger 5} \hat{\sigma}_- + h.c.$

$$\begin{aligned}\chi_{5,e} &= \frac{gR_{-D}\Pi_{11}}{R} + (\text{corr.}) \\ S_{5,e} &= -\mathcal{D}_4\mathcal{D}, \quad \mathcal{D}_4 \equiv \text{sign}(4\omega - 2\delta_+ - R) \\ \varpi_{5,e} &= |4\omega - 2\delta_+ + \mathcal{D}R| \approx |5\omega - \Omega_0 + 2(\delta_- - \delta_+)|,\end{aligned}\tag{12.75}$$

where (corr.) denote additional terms proportional to  $J_2(q)$  and  $J_2(q_2)$ .

In a similar manner one can deduce the resonant frequencies and transition rates for higher-order (odd-photon) exchange and creation transitions, as well as the fractional resonant frequencies  $\varpi_n/k$  due to the nonlinear terms  $\varepsilon^k$ , where  $k$  is an integer [38].

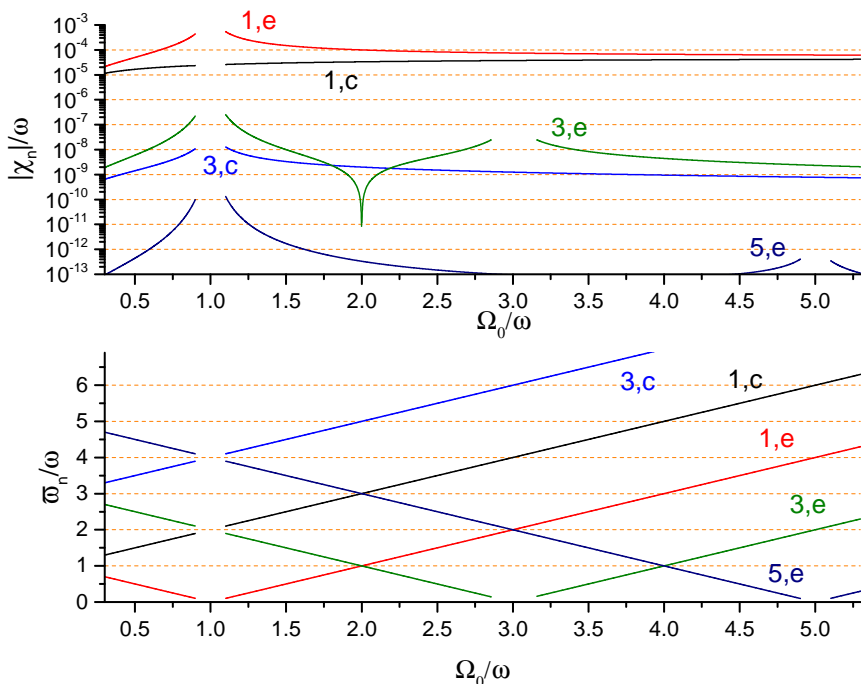


Figure 12.2: Analytic results for the transition rates and resonant modulation frequencies for 1-, 3- and 5-photon exchange and creation transitions. Parameters:  $g = 10^{-2}\omega$  and  $\varepsilon = 10^{-2}\Omega_0$ .

In Figure 12.2 we illustrate the behavior of  $|\chi_n|$  and  $\varpi_n$  [ignoring the terms (corr.) for  $\chi_{3,c}$  and  $\chi_{5,e}$ , therefore evaluating only the order of magnitude of the associated transition rates] as function of  $\Omega_0$  for the five transition discussed above and parameters  $g = 10^{-2}\omega$  and  $\varepsilon = 10^{-2}\Omega_0$  in the region of validity of our approximations ( $\varepsilon \ll \eta$  and  $|\Delta_-| \gg g$ ). Although higher-order resonances are theoretically possible (e. g., 5-photon creation transition or 7-photon resonances) this figure shows that the associated transition

rates would be prohibitively small for the experimental verification, unless  $g$  becomes of the order of  $\omega$ .

### 12.6.1 Linewidth of the resonances

To determine the linewidth of the  $n$ -th resonance one can neglect the dissipation and solve the equations

$$\dot{A}_3 = \chi_n \left( e^{it\mathcal{S}_n(\varpi_n - \eta)} C_3 + c.c. \right) \quad (12.76)$$

$$\dot{C}_3 = -\chi_n (2A_3 - 1) e^{-it\mathcal{S}_n(\varpi_n - \eta)}. \quad (12.77)$$

For the initial condition  $C(0) = A(0) = 0$  (i.e., the initial state  $|\phi_-\rangle\langle\phi_-|$ ) we obtain for the probability of the orthogonal state  $|\phi_+\rangle$

$$A_3(t) = \frac{4\chi_n^2}{(\eta - \varpi_n)^2 + 4\chi_n^2} \sin^2 \left( \frac{t\sqrt{(\varpi_n - \eta)^2 + 4\chi_n^2}}{2} \right). \quad (12.78)$$

Therefore, the maximum value of  $A_3$  is given by the Lorentzian distribution strongly dependent on the modulation frequency  $\eta$

$$A_3^{\max}(\eta) = \frac{1}{1 + \left( \frac{\eta - \varpi_n}{2\chi_n} \right)^2} = \begin{cases} 1 & \text{for } \eta = \varpi_n \\ \frac{1}{2} & \text{for } \eta = \varpi_n \pm 2\chi_n \end{cases}. \quad (12.79)$$

So the half width at half maximum (HWHM) of the resonance is  $2|\chi_n|$ , where  $\chi_n$  is the transition rate at the exact resonance  $\eta = \varpi_n$  [when  $A_3(t) = \sin^2(|\chi_n|t)$ ]. This means that to observe experimentally such transition one needs to adjust the modulation frequency with accuracy  $\lesssim 2|\chi_n|$  around the resonant frequency  $\varpi_n$  and maintain the harmonic modulation during the time interval  $|\chi_n|t \sim \pi/2$ . Besides, the dissipation rates must be small compared to the transition rate:  $\gamma, \gamma_\phi \lesssim |\chi_n|$ .

We emphasize one more time that the deduced resonant modulation frequencies  $\varpi_n$  possess small errors due to the neglected rapidly oscillating terms, because every time one neglects terms of the form  $\alpha e^{it\beta}$  on the RHS of a differential equation, an error  $\sim |\alpha|^2/\beta \times t$  is introduced to the phase of some probability amplitude [see Eq. (12.65)]. But it is usually simpler to find such minor frequency shifts numerically rather than taking into account all the neglected rapidly oscillating terms.

### 12.6.2 Analytic results for the dynamics

For the experimental verification of the  $n$ -th transition the optimal scenario is the exact resonance,  $\eta = \varpi_n$ . Noting that  $\chi_n$  is real, one is left with the equations

$$\dot{A}_3 = \chi_n 2C_3^r e^{-t\Gamma_3} + L e^{-t\Gamma_4} \quad (12.80)$$

$$\dot{C}_3^r = -\chi_n [2A_3 e^{t\Gamma_3} - e^{t\Gamma_5}], \quad (12.81)$$

where  $C_3^r(t) = \text{Re}[C_3(t)]$  and  $C_3^i(t) = \text{Im}[C_3(t)]$ . From the initial conditions (12.66) we have

$$C_3^r(0) = C(0) \cos q, \quad C_3^i(0) = -C(0) \sin q. \quad (12.82)$$

After simplifications, the second-order differential equation for  $C_3^r$  becomes

$$\ddot{C}_3^r - \Gamma_3 \dot{C}_3^r + 4\chi_n^2 C_3^r = -\chi_n \gamma \mathcal{D} (1 - 2\zeta^2) e^{t\Gamma_5}. \quad (12.83)$$

Its exact solution is

$$C_3^r(t) = O_1 e^{t\Gamma_+} + O_2 e^{t\Gamma_-} + O_3 e^{t\Gamma_5}, \quad (12.84)$$

where

$$O_1 = \frac{\chi_n - 2\chi_n A(0) - (\Gamma_5 - \Gamma_-) O_3 - \Gamma_- C(0) \cos q}{\sqrt{\Gamma_3^2 - (4\chi_n)^2}} \quad (12.85)$$

$$O_2 = -\frac{\chi_n - 2\chi_n A(0) - (\Gamma_5 - \Gamma_+) O_3 - \Gamma_+ C(0) \cos q}{\sqrt{\Gamma_3^2 - (4\chi_n)^2}} \quad (12.86)$$

$$O_3 = \chi_n \frac{\mathcal{D}\gamma (1 - 2\zeta^2)}{\Gamma_4 \Gamma_5 - 4\chi_n^2} \quad (12.87)$$

$$\Gamma_{\pm} = \frac{\Gamma_3 \pm \sqrt{\Gamma_3^2 - (4\chi_n)^2}}{2}. \quad (12.88)$$

Finally, integrating (12.80) we find

$$A_3(t) = A(0) - L \frac{e^{-t\Gamma_4} - 1}{\Gamma_4} + 2\chi_n \left[ O_1 \frac{e^{t(\Gamma_+ - \Gamma_3)} - 1}{\Gamma_+ - \Gamma_3} + O_2 \frac{e^{t(\Gamma_- - \Gamma_3)} - 1}{\Gamma_- - \Gamma_3} - O_3 \frac{e^{-t\Gamma_4} - 1}{\Gamma_4} \right]. \quad (12.89)$$

The Figure 12.3 shows the typical behavior of  $e^{-t\gamma_\phi} C(t)$  and  $e^{-t\gamma_\phi} A(t)$  [which characterize the system dynamics, see Eq. (12.15)] according to the analytic solutions (12.82), (12.84) and (12.89) combined with the transformations (12.66) and (12.29). We considered the initial conditions  $A(0) = C(0) = 0$  and the parameters  $g = 10^{-2}\omega$ ,  $\Omega_0 = 1.5\omega$ ,  $n_t = 0.5$ ,  $\varepsilon = 10^{-2}\Omega_0$  and  $\eta = 2\omega - DR + 2\delta_+$  [corresponding to the 1-photon creation transition, Eq. (12.72)], corresponding to the transition rate is  $|\chi_{1,c}| \approx 3 \times 10^{-5}\omega$ . In the panel 12.3a the dissipation rates were  $\gamma = 2 \times 10^{-4}\omega$ ,  $\gamma_\phi = 10^{-4}\omega$  (larger than  $|\chi_{1,c}|$ ), while in the panel 12.3b  $\gamma = 2 \times 10^{-6}\omega$ ,  $\gamma_\phi = 10^{-6}\omega$  (smaller than  $|\chi_{1,c}|$ ). We see that when the transition rate is larger than the dissipative rates the atomic population undergoes damped oscillations; otherwise, the atomic population attains steadily the asymptotic value. For other transitions the behavior is qualitatively similar, since all that matters is the ratio between the transition rate  $\chi_n$  and the dissipative rates.

## 12.7 Conclusions

In this chapter we presented a simple analytic method for deriving the *approximate coarse-grained dynamics* of the semiclassical Rabi model in the presence of Markovian dissipation, when the atomic transition frequency is modulated harmonically by an external agent. We expounded the step by step derivation, so our approach can be easily generalized to include the modulation of other (or multiple) system parameters, nonharmonic perturbations, other dissipative kernels, etc. Closed analytic expressions were obtained for the density operator expanded in the dressed-states basis, confirming the existence of a discrete set

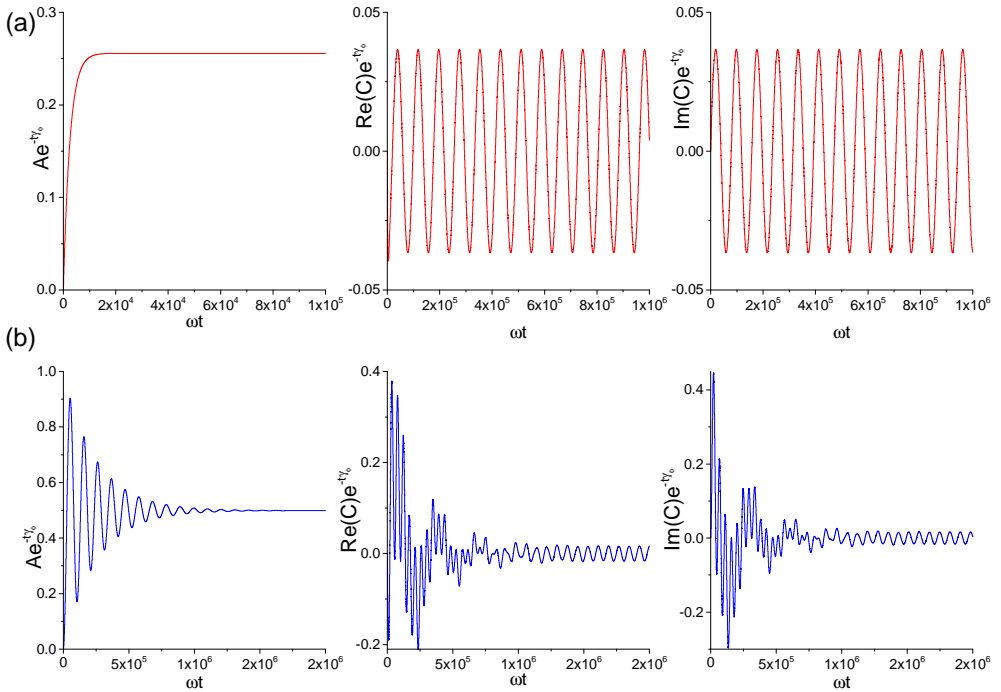


Figure 12.3: Analytic results for the probabilities  $Ae^{-t\gamma\phi}$  and  $Ce^{-t\gamma\phi}$  of the density operator (12.15) for different dissipative rates. In the panel a (b) the dissipative rates are larger (smaller) than the transition rate. See the text for the numerical values of the parameters.

of resonant modulation frequencies for which the atom can be excited from the ground state by a far-detuned classical laser field. Such frequencies are easily explained as  $k$ -photon Jaynes-Cummings or Anti-Jaynes Cummings transitions in the context of the fully quantum formalism, where  $k$  is an odd integer, and the associated transition rates (proportional to the linewidths of the resonances) were derived for  $k = 1, 3, 5$ . Our results show that unless  $g$  is of the order of  $\omega$ , at most 3-photon transitions seem to be within experimental reach.

## Acknowledgment

A. D. acknowledges partial financial support of the Brazilian agencies CNPq (Conselho Nacional de Desenvolvimento Científico e Tecnológico) and Fundação de Apoio à Pesquisa do Distrito Federal (FAPDF, grant number 00193-00001817/2023-43).

## 12.8 References

- [1] Q. Xie, H. Zhong, M. T Batchelor, and C. Lee, The quantum Rabi model: solution and dynamics, *J. Phys. A.: Math. Theor.* **50**, 113001 (2017).

- [2] Daniel Braak, Qing-Hu Chen, Murray T. Batchelor, and Enrique Solano, Semiclassical and quantum Rabi models: in celebration of 80 years, *J. Phys. A: Math. and Theor.* **49**, 300301 (2016).
- [3] D. Braak, Integrability of the Rabi Model, *Phys. Rev. Lett.* **107**, 100401 (2011).
- [4] A. V. Dodonov, Analytical description of nonstationary circuit QED in the dressed-states basis, *J. Phys. A: Math. Theor.* **47**, 285303 (2014).
- [5] I. M. de Sousa and A. V. Dodonov, Microscopic toy model for the cavity dynamical Casimir effect, *J. Phys. A: Math. Theor.* **48**, 245302 (2015).
- [6] A. V. Dodonov, A. Napoli and B. Militello, Emulation of  $n$ -photon Jaynes-Cummings and anti-Jaynes-Cummings models via parametric modulation of a cyclic qutrit, *Phys. Rev. A* **99**, 033823 (2019).
- [7] P. McConnell, A. Ferraro, and R. Puebla, Multi-squeezed state generation and universal bosonic control via a driven quantum Rabi model, Arxiv 2209.07958.
- [8] Q. Bin, Y. Wu, and X.-Y. Lü, Parity-symmetry-protected multiphoton bundle emission, *Phys. Rev. Lett.* **127**, 073602 (2021).
- [9] R. Puebla, J. Casanova, O. Houhou, E. Solano, and M. Paternostro, Quantum simulation of multiphoton and nonlinear dissipative spin-boson models, *Phys. Rev. A* **99**, 032303 (2019).
- [10] A. V. Dodonov, Photon creation from vacuum and interactions engineering in nonstationary circuit QED, *J. Phys.: Conf. Ser.* **161**, 012029 (2009).
- [11] D. S. Veloso and A. V. Dodonov, Prospects for observing dynamical and anti-dynamical Casimir effects in circuit QED due to fast modulation of qubit parameters, *J. Phys. B: At. Mol. Opt. Phys.* **48**, 165503 (2015).
- [12] Y. Lu, S. Chakram, N. Leung, N. Earnest, R. K. Naik, Z. Huang, P. Groszkowski, E. Kapit, J. Koch, and D. I. Schuster, Universal stabilization of a parametrically coupled qubit, *Phys. Rev. Lett.* **119**, 150502 (2017).
- [13] A. V. Dodonov, Continuous intracavity monitoring of the dynamical Casimir effect, *Phys. Scr.* **87**, 038103 (2013).
- [14] A. V. Dodonov and V. V. Dodonov, Dynamical Casimir effect via modulated Kerr or higher-order nonlinearities, *Phys. Rev. A* **105**, 013709 (2022).
- [15] A. V. Dodonov, Dynamical Casimir effect in cavities with two modes resonantly coupled through a qubit, *Phys. Lett. A* **384**, 126837 (2020).
- [16] M. V. S. de Paula, W. W. T. Sinesio and A. V. Dodonov, Ancilla-assisted generation of photons from vacuum via time-modulation of extracavity qubit, *Entropy* **25**, 901 (2023).
- [17] A. V. Dodonov, J. J. Díaz-Guevara, A. Napoli, and B. Militello, Speeding up the antidynamical Casimir effect with nonstationary qutrits, *Phys. Rev. A* **96**, 032509 (2017).
- [18] L. C. Monteiro and A. V. Dodonov, Anti-dynamical Casimir effect with an ensemble of qubits, *Phys. Lett. A* **380**, 1542 (2016).
- [19] H. Dessano and A. V. Dodonov, One- and three-photon dynamical Casimir effects using a nonstationary cyclic qutrit, *Phys. Rev. A* **98**, 022520 (2018).
- [20] A. V. Dodonov, Dynamical Casimir effect via four- and five-photon transitions using a strongly detuned atom, *Phys. Rev. A* **100**, 032510 (2019).
- [21] A. V. Dodonov, D. Valente and T. Werlang, Antidynamical Casimir effect as a resource for work extraction, *Phys. Rev. A* **96**, 012501 (2017).
- [22] A. V. Dodonov, D. Valente and T. Werlang, Quantum power boost in a nonstationary

- cavity-QED quantum heat engine, *J. Phys. A: Math. Theor.* **51**, 365302 (2018).
- [23] C. Cohen-Tannoudji, J. Dupont-Roc, G. Grynberg, *Atom-photon Interactions: Basic Processes and Applications*, Wiley, New York, 1992.
- [24] L. Mandel and E. Wolf, *Optical coherence and quantum optics* (Cambridge university press, 1995).
- [25] E. K. Irish and A. D. Armour, Defining the Semiclassical Limit of the Quantum Rabi Hamiltonian, *Phys. Rev. Lett.* **129**, 183603 (2022).
- [26] I. I. Rabi, On the Process of Space Quantization, *Phys. Rev.* **49**, 324 (1936).
- [27] I. I. Rabi, Space Quantization in a Gyration Magnetic Field, *Phys. Rev.* **51**, 652 (1937).
- [28] F. Bloch, A. Siegert, Magnetic Resonance for Nonrotating Fields, *Phys. Rev.* **57**, 522 (1940).
- [29] L.O. Castaños, Simple, analytic solutions of the semiclassical Rabi model, *Opt. Commun.* **430**, 176 (2019).
- [30] Y. Zhang, E. Lötstedt, and K. Yamanouchi, Population inversion in a strongly driven two-level system at far-off resonance, *J. Phys. B: At. Mol. Opt. Phys.* **50**, 185603 (2017).
- [31] Y. Yan, L. Chen, J. Luo, and Y. Zhao, Variational approach to time-dependent fluorescence of a driven qubit, *Phys. Rev. A* **102**, 023714 (2020).
- [32] I. Sainz, A. García, and A. B. Klimov, Effective and efficient resonant transitions in periodically modulated quantum systems, *Quantum Reports* **3**, 1 (2021).
- [33] I. Sainz, A. B. Klimov, and C. Saavedra, Effective Hamiltonian approach to periodically perturbed quantum optical systems, *Phys. Lett. A* **351**, 26 (2006).
- [34] T. N. Ikeda, S. Tanaka, and Y. Kayanuma, Floquet-Landau-Zener Interferometry: usefulness of the Floquet theory in pulse-laser-driven systems, *Phys. Rev. Res.* **4**, 033075 (2022).
- [35] H. Carmichael, *An open system approach to quantum optics* (Springer, Berlin, 1993).
- [36] W. Vogel and D. -G. Welsch, *Quantum Optics* (Wiley, Berlin, 2006).
- [37] A. V. Dodonov, Novel scheme for anti-dynamical Casimir effect using nonperiodic ultrastrong modulation, *Phys. Lett. A* **384**, 126685 (2020).
- [38] E. L. S. Silva and A. V. Dodonov, Analytical comparison of the first- and second-order resonances for implementation of the dynamical Casimir effect in nonstationary circuit QED, *J. Phys. A: Math. Theor.* **49**, 495304 (2016).

**Cite this work as:**

A. Marinho and A. Dodonov, Analytic approach for dissipative semiclassical Rabi model under parametric modulation, in A. Dodonov and C. C. H. Ribeiro (Eds.), Proceedings of the Second International Workshop on Quantum Nonstationary Systems, pp. 195–210 (LF Editorial, São Paulo, 2024). ISBN: 978-65-5563-446-4.

**Download the entire Book of Proceedings for free at:**

<https://lfeditorial.com.br/produto/proceedings-of-the-second-international-workshop-on-quantum-nonstationary-systems/>